ACS APPLIED MATERIALS & INTERFACES

Research Article

www.acsami.org

pH Dictates the Release of Hydrophobic Drug Cocktail from Mesoporous Nanoarchitecture

Faheem Muhammad,[†] Aifei Wang,[†] Mingyi Guo,[§] Jianyun Zhao,[‡] Wenxiu Qi,[‡] Guo Yingjie,[‡] Jingkai Gu,[‡] and Guangshan Zhu*[,†,⊥]

[†]State Key Laboratory of Inorganic Synthesis and Preparative Chemistry, College of Chemistry, Jilin University, Changchun 130021, China

[‡]College of Life Science, Jilin University, Changchun 130021, China

[§]College of Construction Engineering, Jilin University, Changchun 130021, China

[⊥]Queensland Micro- and Nanotechnology Centre, Griffith University, Nathan, QLD 4111, Australia

Supporting Information

ABSTRACT: Combination therapy has been a norm in clinical practice to effectively treat cancer. Besides polytherapy, nowadays, smart and nanobased drug carriers are extensively being explored to deliver drugs according to pathophysiological environment of diseases. In this regard, herein we designed intelligent mesoporous architecture, incorporating both combinational therapy with smart nanotechnology, to simultaneously deliver two highly hydrophobic chemotherapeutic drugs in response to extracellular and/or intracellular acidic environ of tumor. Novelty of the system lies in the employment of acid responsive ZnO QDs to clog not only the nanochannels of mesoporous silica, encapsulating one hydrophobic drug, but also exploitation of chelate forming propensity of another hydrophobic drug (curcumin) to load a significant quantity onto the surface of ZnO nanolids. Cell viability results revealed an extraordinarily high cytotoxic efficiency of that lethal drug cocktail even at a concentration as low as 3 μg/mL nanocarrier. We envision that this sophisticated nanocarrier, which utilizes both interior pore and exterior surface of nanolids for loading different hydrophobic guest molecules and their subsequent acid responsive release, will undoubtedly, illustrates its remarkable potential in targeted chemotherapy.

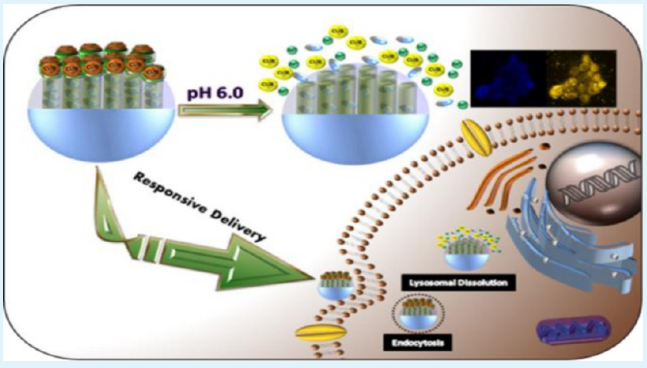

KEYWORDS: *Chemotherapy, controlled release, curcumin, mesoporous silica, stimuli responsive*

1. INTRODUCTION

Recently, cancer has gained a status as one of the leading health risk in terms of mortality, morbidity and economic costs. Medical community has, in this regard, made great strides to tackle this haunting spectre through addressing the molecular underpinnings responsible for this complex disease.[1−4]Despite those substantial developments, death rates from cancer have unfortunately not altered over the decades.[5] Chemotherapy has been a standard cancer treatment, which indiscriminately target actively dividing cells throughout the body. This nontargeted onslaught inevitably results in the killing of not only cancer cells, but also healthy ones come under attack. Water solubility and drug resistance poses further terrific challenges for effective cancer therapy. Intensive research efforts have been dedicated toward the development of targeted and smart drug carriers in order to efficiently combat all these obstacles. Luckily, advancement in the nanotechnology in recent times also has proven a great boon for oncology, because of well-established passive targeting capability of nanoparticles.[1−6] With time, a plethora of sophisticated nanoparticle-based drug delivery systems has been engineered to ferry cytotoxic drugs or therapeutic genes into malignant cells, without harming healthy cells. Notably, all of those nanoplatforms mostly carry one drug; however, in clinical practice, multiple drugs are routinely prescribed to effectively treat cancer. The driving force for the clinical preference and established high efficacy of combination therapy is actually the development of synergy among the different drugs and prevention of drug resistance, which is considered a leading cause of chemotherapy failure. It should also be kept in mind that the use of multiple drugs is indeed escorted with more life-threatening side effects; thus, there is substantial need to integrate combinational therapy with nanotechnology. Researchers and clinicians are now working together to design such a nanoarchitecture which are capable of loading multiple cytotoxic drugs, with different solubilities and working mechanism, into a single nanocarrier.[7]

Received: August 20, 2013
Accepted: October 18, 2013
Published: October 18, 2013

Scheme 1. Schematic Presentation of Synthetic and Working Protocol of Multiple Drug Ferrying pH Responsive and Controlled Drug Release System

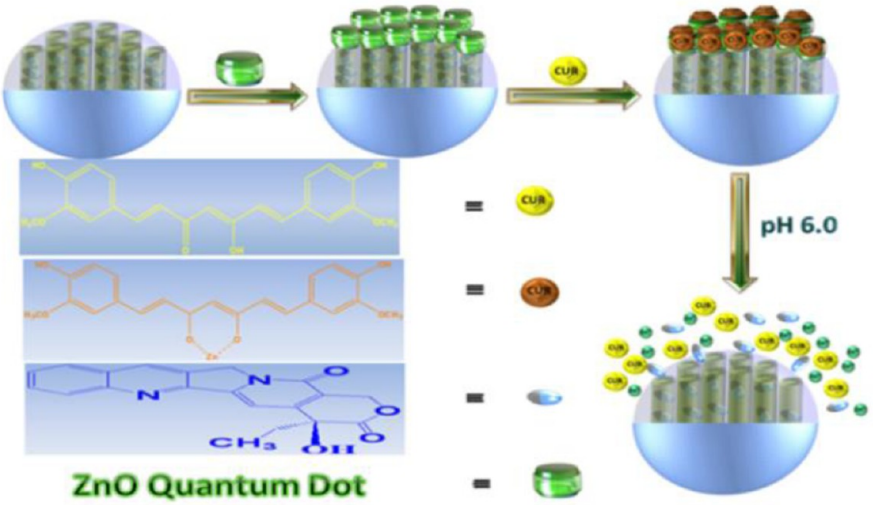

Among all the available nanoplatforms, mesoporous silica nanoparticles (MSNs) have been increasingly explored as promising vehicles for intracellular drug delivery, mainly because of their excellent biocompatibility and high surface area.[8−10] Besides a highly porous structure for efficient drug loading, the ease with which we introduce organic moieties onto the surface of MSNs really empowers us to exploit it for variety of other biomedical applications. For instance, mesoporous silica has been widely demonstrated as stimuli responsive drug delivery vehicle to minimize the premature release of cytotoxic drugs by manipulating diverse kinds of gatekeepers. Varieties of extrinsic and intrinsic triggers have been tried to regulate the release of cargo molecules.[11−13] However, in relation to chemotherapy, pH responsive nanoparticles are highly necessitated due to the existence of slightly acidic pH value (pH 6.5−7.0) of inflamed tissues, primary tumors, and metastasized tumors, compared with normal tissues (pH 7.4). Aberrant glycolytic metabolism actually contributes to the mildly acidic environment of cancer cells. Moreover, after endocytosis, reduction in pH from endosomes to lysosomes can similarly serve as a trigger for intracellular drug release. To date, number of MSNs based pH responsive nanodevices, capable of releasing cargo in acidic microenvironment, has been reported.[14] Aznar et al. introduced an acid responsive feature by functionalizing the outlet of nanochannels with boron ester bonds.[15]The hydrolysis of this bond at relatively low pH (∼3) led to the opening of pores to permit the release of cargo molecules. Feng et al. later reported a pH-responsive nanogated ensemble by linking gold nanoparticle onto the surface of mesoporous silica through acid labile acetal group.[16] Stoddert's group also developed a number of pH sensitive nanovalves to regulate the cargo release in MSNs, using supramolecular chemistry.[17−19] Recently, pH-sensitive hydrazone bond was used to directly link anticancer drug with MSNs framework.[20] More recently, we reported a pH receptive gated system wherein ZnO quantum dots (QDs) were employed as nanolids to avoid the premature release of a cytotoxic drug.[21] All of the reported pH responsive systems transport just one drug at a time, and till now MSNs have rarely been used as a stimuli responsive nanocarrier for multiple chemotherapeutic drugs. Our previous study has driven us to develop a stimulus responsive multiple drug carrying nanoparticles, which could integrate the exclusive advantages of multiple drugs with nanoparticle-based targeted drug delivery. Herein we report a straightforward strategy to engineer a smart mesoporous architecture that integrates combinational therapy with nanotechnology to simultaneously deliver two hydrophobic cytotoxic drugs, having different mode of actions, in response to extracellular and/or intracellular acidic milieu of cancer cells. This ingenious approach first achieves the loading of campothetacin (topoisomerase I inhibitor) into the nanopores of amine functionalized MSNs. To ensure the minimum release of campothetacin before reaching the targeted sites, mesoporous silica nanoparticles are capped with acid sensitive ZnO QDs. Subsequently, another cost-effective multipurpose drug (curcumin) is additionally loaded onto ZnO nanolids with an objective to achieve acid responsive multidrug delivery in pancreatic cancer cells. ZnO QDs in this study simultaneously acts as nanocaps to block the release of encapsulated drug and provides conjugating site for loading another highly hydrophobic drug via coordinate bond (Scheme 1). Drug release profile demonstrates an efficient burstlike release behavior of curcumin, whereas CPT is released in a controlled fashion but after the dissolution of ZnO nanolids in response to mildly acidic conditions.

2. EXPERIMENTAL SECTION

2.1. Synthesis of Mg-Doped ZnO Quantum Dots. ZnO QDs were prepared using a previously reported protocol with a slight modification. Zinc acetate (550 mg, 2.5 mmol) and magnesium acetate (56 mg, 0.25 mmol) were dissolved in boiling ethanol (30 mL) under vigorous stirring. In a separate flask, NaOH (120 mg, 3.5 mmol) was dissolved in refluxing ethanol (10 mL). The salt solutions were then cooled down in ice bath. The ethanolic NaOH was later quickly injected into the former flask. The mixture was stirred for 8 h for particles growth and the resulting transparent quantum dots dispersion displayed an intense green emission, under UV lamp excitation at 365 nm. Finally, ZnO quantum dots were precipitated using hexane as a nonsolvent.

2.2. Synthesis of Amine-Capped ZnO QDs. Precipitated ZnO QDs (100 mg) were dispersed in anhydrous N,N-dimethylformamide (DMF, 20 mL) under sonication to again obtain a transparent solution. 3-aminopropyltriethoxysilane (50 μL) was then added into the DMF solution. The reaction mixture was stirred at 130 °C for 20

min. The precipitated amine-functionalized ZnO QDs were isolated by centrifugation. The wet ppt of ZnO-NH_2QDs was subsequently dispersed in water to get transparent water stable quantum dots.

2.3. Synthesis of Mesoporous Silica Nanosphere. Following a previously reported procedure, mesoporous silica nanoparticles were synthesized.[6] First, CTAB (1.0 g, 2.7 mmol) was dissolved in 480 mL of nanopure water. Sodium hydroxide aqueous solution (2.00 M, 3.5 mL) was introduced into the CTAB solution and the temperature of the mixture was increased to 80 °C. After attaining the desired temperature, TEOS (5.0 mL, 22.4 mmol) was added dropwise to the above alkaline surfactant solution under vigorous stirring. The mixture was allowed to stir for 2 h to produce a white precipitate. The resulting solid crude product was filtered, washed with nanopure water and ethanol, and dried at 60 °C.

2.4. Synthesis of Carboxylic Acid-Functionalized MSNs (MSNs-COOH). In order to functionalize the outer surface of MSNs with carboxyl group, as-synthesized MSNs (1 g) were suspended in 50 mL of dry toluene, containing 1 mL of APTES. The solution was stirred under reflux for 12 h. The functionalized sample was washed with ethanol and water. Subsequently, 300 mg of amine-functionalized MSNs was added into 15 mL of Dimethylsulfoxide (DMSO) solution, containing succinic anhydride (150 mg) and triethylamine (100 mg), and stirred the suspension at 55 °C for 24 h to obtain MSNs-COOH. Acid treatment was later carried out to remove the surfactant template (CTAB) by dispersing MSNs-COOH nanoparticles in 100 mL of methanolic solution containing 0.5 g of NH_4NO_3. The suspension was reflux at 70 °C for 12 h. The final product was centrifuged and washed with ethanol trice.

2.5. Loading, Capping, and Release Experiments. For loading hydrophobic camptothecin (CPT) in the nanopores of MSNs, carboxylic functionalized nanoparticles (50 mg) were introduced into DMSO solution of camptothecin (5 mL, 1 mg mL^{-1}) and stirred for 12 h. Later, the above solution was dispersed in 30 mL of water and further stirred for 6 h. After loading, the solution was centrifuged and washed with PBS. To cap the CPT-loaded COOH-MSNs, we dispersed the powder in water, and then added 15 mg of EDC and 5 mL of ZnO-NH_2 aqueous solutions (10 mg mL^{-1}) . The mixture was stirred for 10 min and afterward centrifuged to remove extra ZnO QDs. One day additional stirring was required to release extra drug from uncapped nanopores. In the end, precipitate was centrifuged, washed several times with water (pH 7.0). The loading quantity of CPT (0.17 mmol g^{-1}) was calculated by using UV/Visible spectroscopy. Another drug Curcumin (CUR) was conjugated onto ZnO QDs and its loading amount (0.20 mmol g^{-1}) was similarly calculated via UV/vis spectroscopy using 425 nm wavelengths. Capping protocol was probed by studying the release profiles of one and two drugs ZnO@MSNs formulations in three different media (acetate buffer; pH 5.0; 6.0 and pH 7.4), using a dialysis bag diffusion technique. Briefly, 10 mg of CPT and curcumin loaded ZnO@MSNs formulations were dispersed in 5 mL of different buffer solutions with a few drops of ethanol, after one minute the samples were centrifuged and calculate the amount of released curcumin at different pH. To determine the release behavior of CPT, which was loaded inside the nanopores, all samples were redispersed in 3 mL of PBS buffer solutions and sealed in a dialysis bag (molecular weight cutoff = 8000). The dialysis bag was in turn submerged in 20 mL of PBS solutions and stirred for 7 days. The released cargo molecules in the buffer were collected at predetermined time intervals and analyzed by UV/vis spectroscopy.at 365 nm and 425 nm, respectively.

2.6. Cell Culture. BxPC-3 (Pancreatic cancer cell line) were grown in monolayer in Dulbecco's Modified Eagle's Medium (DMEM, Gibco) supplemented with 10% (v/v) fetal bovine serum (FBS, Tianhang bioreagent Co., Zhejiang) and penicillin/streptomycin (100 U mL^{-1} and 100 μg mL^{-1}, respectively,) in a humidified 5% CO_2 atmosphere at 37 °C.

2.7. Cell Viability. The viability of cells in the presence of nanoparticles were evaluated using 3-[4,5-dimethylthialzol-2-yl]-2,5-diphenyltetrazolium bromide (MTT, Sigma) assay. The assay was carried out in triplicate in the following manner. For MTT assay, BxPC-3 cells were seeded into 48-well plates at a density of 8×10^3 per well in 100 μL of media and grown overnight. The cells were then incubated with various concentrations of ZnO@ MSNs, CPT-ZnO@ MSNs, CUR -ZnO@MSNs and CUR-CPT-ZnO@MSNs formulations for 48 h. Afterward, cells were incubated in media containing 0.5 mg mL^{-1} of MTT for 4 h. The precipitated formazan violet crystals were dissolved in 100 μL of 10% SDS in 10 mmol HCl solution at 37 °C overnight. The absorbance was measured at 570 nm by multidetection microplate reader (Synergy TM HT, BioTek Instruments Inc., USA).

2.8. Confocal Laser Scanning Microscopy (CLSM). To check cellular uptake and release of both drugs, BxPC-3 cells were cultured in an 12-well chamber slide with one piece of cover glass at the bottom of each chamber in incubation medium (DMEM) for 24 h. Double drug ZnO@MSNs formulations were added into the incubation medium at the concentration of 50 and 100 μg mL^{-1} for 4 h incubation in 5% CO_2 at 37 °C. After the medium was removed, the cells were washed twice with PBS (pH 7.4) and the cover glass was visualized under a laser scanning confocal microscope (FluoView FV1000, Olympus).

3. RESULTS AND DISCUSSION

Amine functionalized mesoporous silica nanoparticles (MSNs-NH_2) were first synthesized according to a previously established method. Post grafting strategy was employed to introduce amine moiety for further modification. The surface of MSNs was afterward modified with carboxylic groups to assist in the blocking of drug loaded nanochannels, using ZnO nanolids.Transmission electron microscopy (TEM) and scanning electron microscopy (SEM) micrographs (Figure 1)

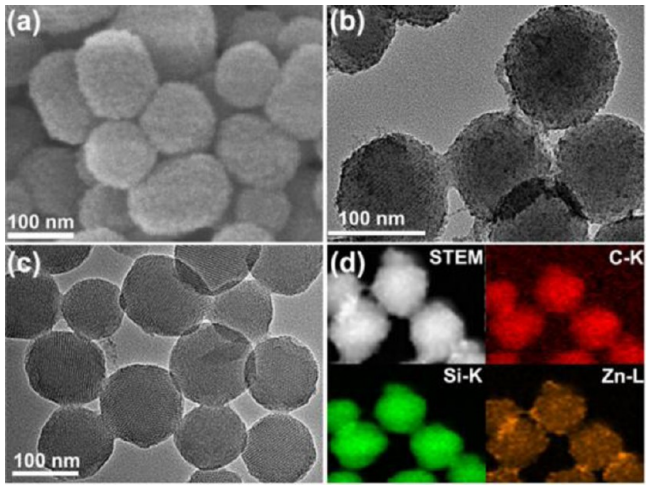

Figure 1. (a) SEM and (b) TEM micrographs of drug-loaded, ZnO-capped MSNs. (c) TEM micrograph obtained after exposing sample to pH 6.0, demonstrating the dissolution of the ZnO nanolids. (d) Element mapping of Si, O, and Zn, confirming the presence of ZnO nanolids in ZnO@MSNs.

reveals as-synthesized sphere-shaped MSNs with a diameter of ~100 and 2.2 nm wide hexagonally arranged pores. Nitrogen adsorption analysis provides the surface area of MSNs-NH_2, which is found to be 857 m^2 g^{-1} (see Figure S3 in the Supporting Information) .Such a large surface area of MSNs is exploited to load hydrophobic drug inside the nanochannels. The synthesis of water-dispersible ZnO QDs was carried out by treating QDs with organosilane 3-aminopropyltriethoxysilane (APTES) in DMF. The resulting luminescent amine-functionalized ZnO QDs (denoted as ZnO-NH_2) are of 3−4 nm in size, and well-characterized by TEM, energy-dispersive spectroscopy (EDS) analysis, and FTIR spectroscopy (see Figures S1 and S5 in the Supporting Information). Proof-of-concept study was performed by loading a model hydrophobic anticancer drug,

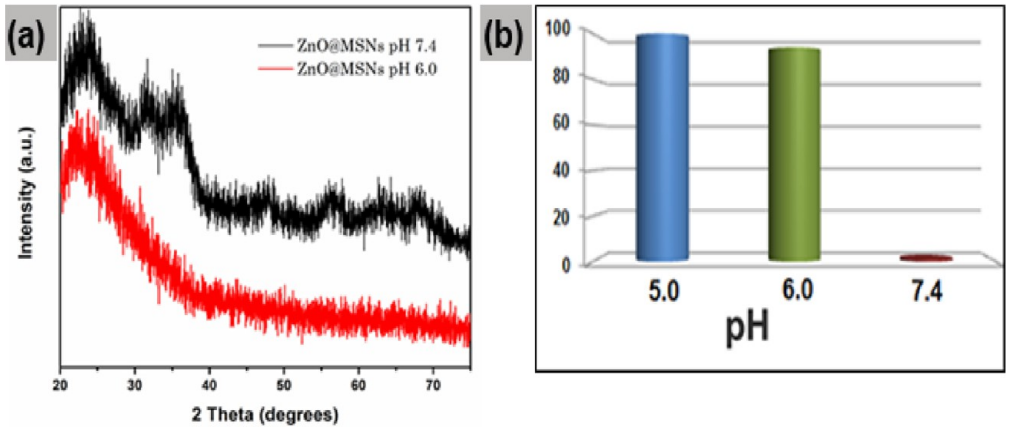

Figure 2. (a) High-angle XRD patterns of ZnO@MSNs at pH 7.4 and 6.0, which clearly illustrates the dissolution of ZnO nanolids in mildly acidic conditions. (b)ICP-OES data demonstrates the dissolution of ZnO nanolids from ZnO@MSNs formulation in different pH buffer solutions.

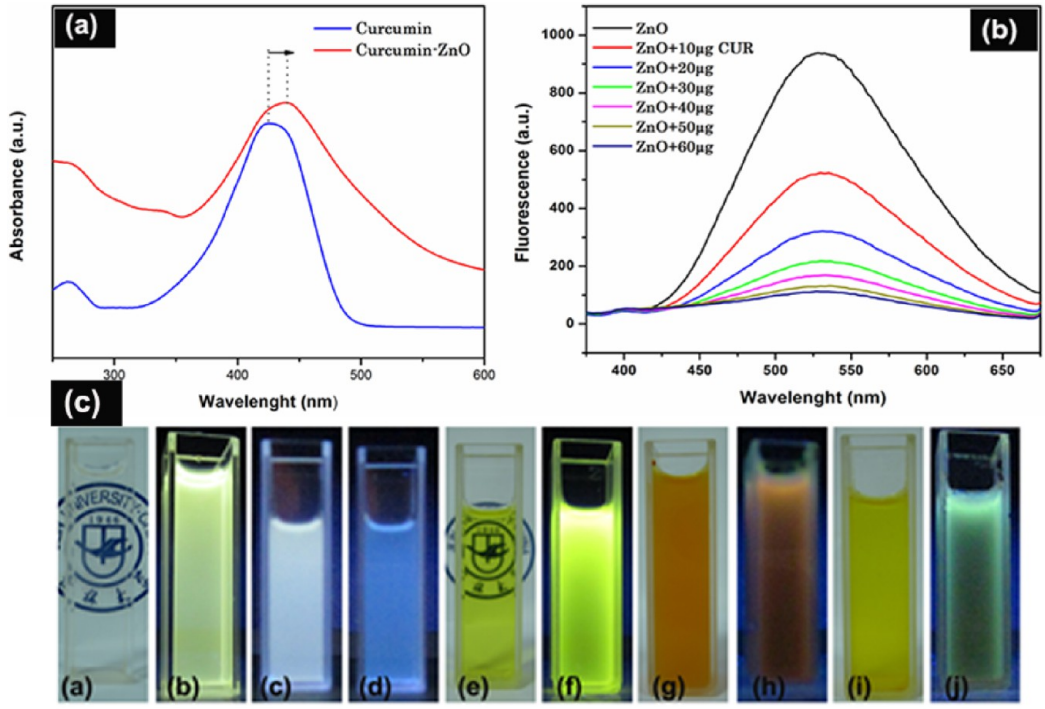

Figure 3. (a) Absorbance spectra of free curcumin (blue) and CUR-ZnO QDs (red) in ethanolic solutions. (b) Fluorescence spectra of ZnO-NH_2 QDs with increasing curcumin concentration from 0, 10, 20, 30, 40, 50, 60 μg (top to bottom). The excitation wavelenth is 350 nm and the pH is 7.0. (c) Photograph (a) under white light, ZnO-NH_2 QDs in water. (b) Under UV light, ZnO-NH_2 in water. (c) Under UV light, CPT-ZnO@MSNs at pH 7.0. (d) Under UV light, CPT-ZnO@MSNs at pH 6.0. (e) Under white light, ethanolic solution of curcumin. (f) Under UV light, ethanolic solution of curcumin. (g) Under white light, CUR-CPT-ZnO@MSNs at pH 7.0. (h) Under UV light, CUR-CPT-ZnO@MSNs at pH 7.0. (i) Under white light, CUR-CPT-ZnO@MSNs at pH 6.0. (j) Under UV light, CUR-CPT-ZnO@MSNs at pH 6.0.

camptothecin (CPT), into the pores of MSNs-COOH. Considerably large amount of CPT was loaded into the nanochannels of MSNs, the loading amount was found to be 62 mg/g. After loading CPT, the nanochannels of the MSNs-COOH nanocarriers were clogged with ZnO−NH_2 QDs with the aid of EDC chemistry. Finally, curcumin was successfully loaded onto the surface of ZnO capped MSNs. UV−vis absorption spectroscopy was used to evaluate the loading amountof curcumin, which indicated a fairly high dose of drug loading (7.4%). Since, quinone and phenol moieties exhibits a pronounced affinity toward divalent metal ions, that is why, transition metal (Zn^{2+}) in this study ensured the loading of curcumin via chelation.[22] As mentioned above, mesoporous silica has undoubtedly been reported as hydrophobic drugs carrier, but actually it always carried one drug at a time, it has never been explored for the delivery of two hydrophobic drugs simultaneously in response to environmental conditions. This strategy, for the first time, make sure the delivery of two hydrophobic drugs using mesoporous silica as nanocarrier, and especially in response to pathophysiological trigger.The successful capping of CPT loaded MSNs was corroborated by number of characterization techniques. Compared to as-synthesized MSNs, SEM and TEM micrographs of CPT-ZnO@MSNs (Figure 1a,b) indicates a substantial capping of MSNs pores to minimize the premature leakage of cytotoxic drugs, as shown by numerous distinguishing dark crystalline

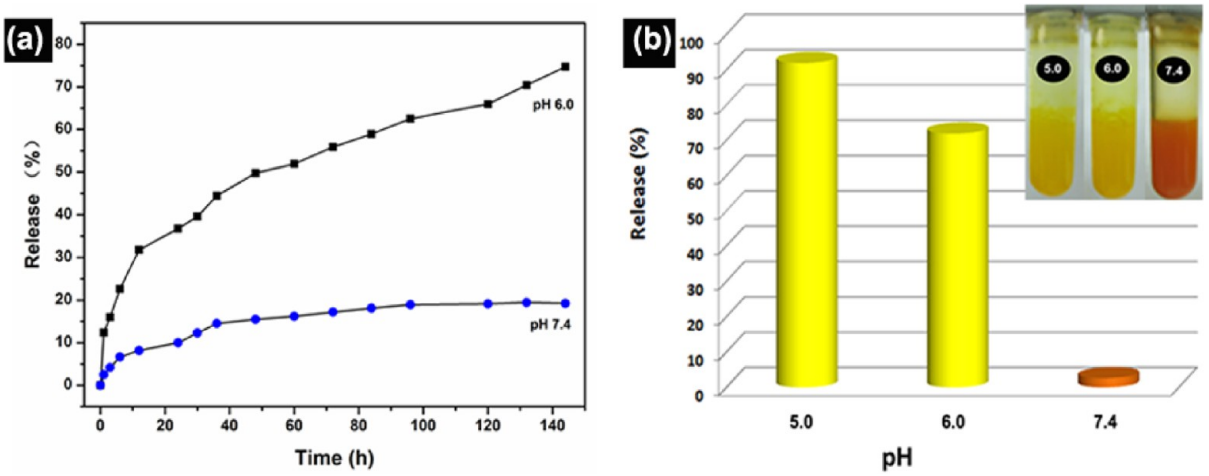

Figure 4. (a) Release profile of camptothecin from CUR-CPT-ZnO@MSNs nanoformulaton at pH 7.0 and pH 6.0. (b) Release profile of curcumin from CUR-CPT-ZnO@MSNs at pH 7.4, 6.0 5.0. Inset: respective photographs of double drug nanoformulations at different pH (3 mg/mL), indicating the extent of curcumin release over one minute. The release of drug molecules was monitored by UV−Vis spectrophotometer.

spots of 3−4 nm on the surfaces of the MSNs. The energy-dispersive X-ray spectroscopy (EDX) mapping analysis also validated a significant and uniform capping of drug loaded nanopores using ZnO QDs, as shown in Figure 1d. Compositional analysis of capped MSNs endorses the presence of elemental signal of zinc. In addition to zinc, signal of silicon and oxygen and carbon are also detected. To obtain further evidence for endorsing the presence of ZnO QDs in MSNs formulation, the XPS analysis was performed. Figure S4 in the Supporting Information illustrates the survey spectrum for ZnO@MSNs along with high-resolution spectra in the binding energy regions for Si 2p, O 1s, Zn 2p, and C 1s photoelectrons,and peaks around 102.9, 532.2, 1021.9, and 284.5 eV are correspondingly detected. In two peaks at a binding energy of 1021.9 and 1045.0 eV in the Zn 2p region are assigned to Zn^{2+} in ZnO crystals. Reduction in surface area and decrease in the intensity of the (100) XRD peak also indicates the successful capping of drug charged nanochannels (see Figure S2,3 in the Supporting Information). To authenticate the dissolution of ZnO QDs at pH 6.0, TEM analysis again came to play (Figure1c). Evidently, the exposure of CPT-ZnO@MSNs to acetate buffer solutions (pH 6.0) triggers a complete dissolution of nanolids, and as a result QDs are not found whatsoever on the surface of MSNs, confirming the instant disintegration of ZnO QDs in mildly acidic medium. ICP-OES data (Figure 2b) also shed some light on the dissolution of ZnO. Wide-angle powder X-ray diffraction (XRD) patterns of ZnO@MSNs similarly provides a convincing proof of the existence and dissolution of ZnO as revealed in Figure 2a.

Generally, drugs are loaded into nanocarriers by utilizing weak noncovalent interactions, such as, physical adsorption, electrostatic interaction and $\pi-\pi$ stacking, and subsequently their release is accomplished by breaking these labile bonds between the host and guests. Metal ion−ligand interactions have scarcely been used to load drugs in nanocarriers. In this study, coordination chemistry was exploited to efficiently load another drug (curcumin) onto ZnO nanolids. Interaction between divalent transition metal ions and curcumin is clearly visible from the color change of curcumin solutions as illustrated in Figure 3c. The color of CPT loaded MSNs was remarkably altered from off-white to intense orange after curcumin loading, because of the formation of metal complex. Previously, several studies have been reported regarding the complexation of anthracyclines drugs by metal ions, which is mainly attributed to the presence of electron-rich acetylacetone, hydroxyl, and even, in some instances, the amino groups.[23−25] Absorption and fluorescence techniques facilitated to validate the interaction between curcumin and metal ions. After chelation, red shift in the absorption maximum of curcumin from 425 to 440 nm was detected, suggesting the deprotonation of hydroxyl and conjugation of quinone groups by the metal ions (Figure 3a). Likewise, fluorescence quenching of ZnO QDs also indicated its successful loading onto the ZnO surfaces via complexation. Prior to this interaction, both curcumin and ZnO nanolids were luminescent, but coordination-mediated binding of curcumin with ZnO QDs resulted in highly efficient quenching of both species as revealed in Figure 3b and photographs in Figure 3c. Furthermore, the surface modification and loading of drugs were confirmed by Fourier transform infrared (FTIR) spectroscopy (see Figure S5 in the Supporting Information). As far as curcumin loading goes, the band at 1580 cm^{-1} refers to the stretching vibration of carbonyl groups of curcumin, suggesting the successful loading of curcumin.

To prove the concept of pH responsive release of two drugs, different MSNs formulations were incubated in water and acetate buffers (pH 6.0) to evaluate the released quantities of both drugs, using UV/Visible spectroscopy. First, the release pattern of one drug formulation (CPT-ZnO@MSNs) was evaluated. At physiological pH, the ZnO nanolids were found to be quite stable and remained intact, consequently, relatively low CPT leakage was observed from the silica nanoreservoir as reveled in Figure 4a. On the contrary, exposure to slightly acidic environ inevitably resulted in a rapid disintegration of ZnO nanolids that in turn opens the mesopores to release entrapped CPT molecules. Lowering the pH to 6.0, mimicking the extracellular tumor environment, triggered a considerable release of CPT. It was found that almost 100% of the nanolids were suddenly dissolved from the outlets of nanopores, as confirmed earlier, led to complete opening of pores and accordingly CPT molecules started releasing in a controlled fashion. Second, release profiles of two drug nanoformulation (CUR-CPT-ZnO@MSNs) was similarly determined at differ-

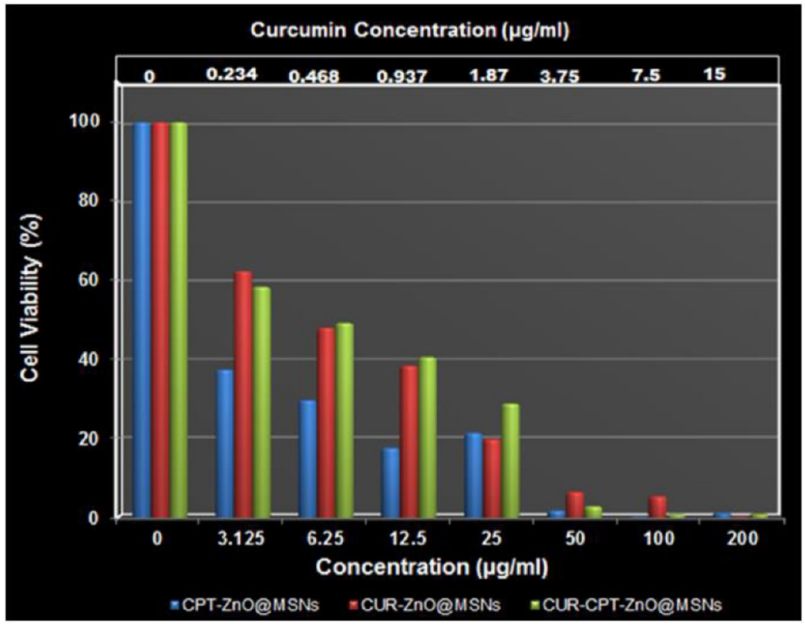

Figure 5. In vitro viability of BxPC-3 cells in the presence of different concentrations of CPT-ZnO@MSNs, CUR-ZnO@MSNs, and CUR-CPT-ZnO@MSNs; the incubation time was 48 h.

ent pH levels. Expectedly, two drug formulations displayed almost negligible release of both drugs, due to the capping of pores and stability of CUR-metal complex at pH 7.0. Only ∼15% of CPT and 3% curcumin were released after 6 days incubation. Apart from the stability of ZnO at physiological pH, the dative bond between Zn^{2+} and curcumin is also quite stable at pH 7.0, as a result, no drug release was observed at neutral pH. Mechanistically,since chelation is a pH dependent phenomenon, thus, formation and cleavage of metal ion−ligand coordination bonds mainly rely on pH changes due to intense competition between metal ions and protons (H^+) (Lewis acid) to bind with the ligand (Lewis base). Stability of Zn^{2+}-CUR bond is quite low at mildly acidic pH due to the protonation of the phenolic and ketonic groups of curcumin responsible for conjugation. Hence, exposing the CUR-CPT-ZnO@MSNs sample to pH ∼6.0 resulted in a considerable burstlike release of curcumin (∼70%) from the surface of nanolids, whereas further lowering the pH value to 5.0 led to an instant and complete release of surface bound curcumin molecules(Figure 4b). The cleavage of drug-metal bond is clearly depicted in color change of bound curcumin from intense orange to yellow, suggesting the release of yellow colored curcumin molecules (inset of Figure 4b). Furthermore, ZnO nanolids are dissolved at the same time, as already established from TEM and other examinations. After the release of surface bound curcumin and disintegration of nanolids, CPT molecules find no hindrance in their way to be released in a sustained way from the nanopores. Release profile confirms the double role of ZnO nanolids which on the one hand clog the CPT-loaded nanopores and on the other hand chelate with curcumin, subsequently requiring acidic environments for successful and sufficient release of both drugs. Taken together, these results clearly validates a time and pH dependent release of CPT, whereas, curcumin exhibited a burstlike release behavior in response to acidic environ. This kind of pH sensitive dual drug delivery can be especially suited for minimizing off-target side effects of anticancer drugs.

To verify the pharmacological activity of double drug nanocarrier, we carried out MTT assay, wherein the viability of pancreatic cancer cells (Bxpc-3) cells was evaluated upon incubating various concentrations of different MSNs formulations for 48 h (Figure 5). The cell proliferation activity was not hindered at all, when cells were exposed to ZnO@MSNs formulation (without any drug) to as high as 100 μg/mL, fulfilling the prerequisite for a nanocarrier to be biocompatible. However, CPT-ZnO@MSNs nanoformulation showed an exceptionally high dose dependent anticancer activity. Around 65% of cell reduction was achieved at the particle concentration of just ∼3 μg/mL nanoformulation, whereas the corresponding concentration of CPT free ZnO@MSNs formulation was unable to cause any cell damage at such a low dose. This cytotoxicity of CPT containing formulation was consistent with the in vitro drug release data, which suggested a sustained pH sensitive release of CPT from ZnO@MSNs for the sake of comparison, curcumin containing ZnO@MSNs formulation was also tested, which likewise resulted in a significant decrease in cell viability in a concentration-dependent manner, with a (IC_{50}) value of less than ∼6 μg/mL drug formulation. Unexpectedly, two drug formulations at low drug concentrations exhibited a slightly less inhibiting capacity against the cell proliferation than either CPT or curcumin alone, possibly because of antagonistic effect, but at higher concentrations all drug formulations proved to be extremely lethal. It is worth mentioning that curcumin was loaded onto the surface of nanocarrier and exhibited a burstlike release behavior, therefore, it presumably works as an antioxidant initially against slowly releasing CPT molecules, but with increasing time, a sustained release of CPT molecules from the nanochannels of MSNs consequently caused the apoptosis of cancer cells. Considering antioxidant property of curcumin, as chemotherapy normally end up with severe cardiotoxicity due to excessive generation of reactive oxygen species, hence antioxidant property of curcumin can also be highly beneficial in mitigating the negative effects of chemotherapy. The IC_{50} value of double drug formulation (CUR-CPT-ZnO@MSNs) against cancer cells was similarly as

low as ~6 μg/mL, thus, suggesting a significant potential of this multidrug nanocarrier in chemotherapy. When compared to other stimuli responsive systems, this two drugs ferrying ZnO capped nanoparticles ensures significantly high encapsulation of two hydrophobic drugs, tunable and sustained drug release over a longer period of time in case of CPT, and excellent pH responsive release behavior of curcumin, which is evident from cytotoxicity data.

Efficient cell uptake of nanocarriers is inevitably linked with efficacious chemotherapy, therefore, cellular uptake and intracellular release of multiple drugs was evaluated by using confocal laser scanning microscopy (CLSM). Different MSNs based formulations were incubated with pancreatic cancer cell line (Bxpc-3). To test the dissolution of luminescent ZnO QDs, we first incubated ZnO@MSNs for 30 min, and weak yellowish green spots in the cytoplasmic region clearly indicated a successful internalization of ZnO-capped MSNs. Three hours later, images showed no luminescence; the quenching of ZnO QDs most probably is a result of dissolution of nanolids in mildly acidic conditions (see Figure S6 in the Supporting Information). To visualize the internalization of drugs loaded ZnO@MSNs formulations, the innate fluorescent nature of both curcumin (yellow fluorescence) and CPT (blue fluorescence) was efficiently exploited. Blue emission in the cells (Figure 6b) suggests the intracellular release of CPT from

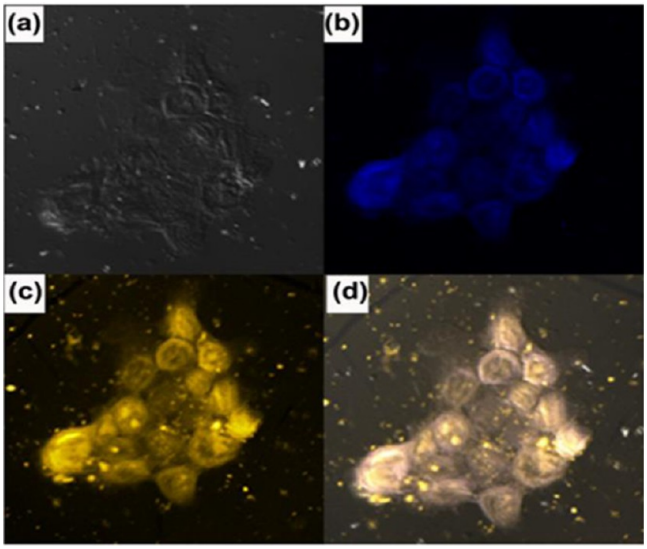

Figure 6. CLSM micrographs of BxPC-3 cells after 4 h incubation with CUR-CPT-ZnO@MSNs (50 μg/mL): (a) transmission image of cancer cells, (b) blue fluorescence indicates the release of CPT from nanoformulation after ZnO dissolution (excitation 405 nm), (c) yellow fluorescence shows the release of curcumin (excitation 488 nm), (d) overlaid image (b and c) indicates the intracellular release of both drugs.

CUR-CPT-ZnO@MSNs, after acid responsive dissolution of ZnO nanolids. As for as double drugs formulation is concerned, before releasing CPT molecules from nanochannels, first of all CUR-Zn^{2+} chelate dissociation and ZnO nanolids dissolution should be transpired in response to acidic environment of endosomal/lysosomal compartments. Expectedly, both blue and yellow fluorescence are emitted simultaneously in the cytoplasmic region of cancer cells after 4 h incubation, signifying the successful intracellular release of two drugs via complex cleavage and nanolids dissolution. The overlay of the bright field and fluorescent images further validates the intracellular delivery of two fluorescent drugs, and it can be seen that fluorescence is strongly localized within cytoplasm and subcellular vesicles from where they target different mechanisms to tackle cancer machinery. On the basis of in vitro results, we corroborated the acid-triggered release of a drug cocktail from mesoporous silica nanoparticles that can potentially be highly advantageous, while considering the acidic cancer microenvironment or acidic cellular compartments of cancer cells.

CONCLUSIONS

In conclusion, we have developed a truly intelligent mesoporous architecture, incorporating combinational therapy with nanotechnology, to simultaneously deliver two hydrophobic chemotherapeutic drugs, in response to extracellular and/or intracellular acidic environ of tumor. Distinctiveness of the system lies in the employment of acid responsive ZnO QDs to clog not only the nanochannels of mesoporous silica, encapsulating one hydrophobic drug, but also exploitation of chelate forming propensity of curcumin to load a significant quantity onto the surface of ZnO nanolids. Drug cocktail, intended for different targets, was well retained and minute off-target leakage was observed at physiological pH, whereas exposure to mildly acidic milieu triggered the dissolution of ZnO nanolids, resulting in an instant burst-like release of curcumin and controlled release of CPT molecules from MSNs channels .Cell viability results confirmed the extraordinarily high cytotoxic efficiency of that lethal double drug combination even at a concentration as low as ~3 μg/mL nanocarrier. Confocal images also verified the acid sensitive intracellular release of drugs cocktail. We anticipate that this sophisticated nanocarrier, which utilizes both interior pore and exterior surface of nanolids for loading different hydrophobic guest molecules and their subsequent acid responsive release, will undoubtedly illustrate its remarkable potential in targeted chemotherapy.

ASSOCIATED CONTENT

Supporting Information

Materials, characterization of nanolids and resulting nanoformulation, and confocal images. This material is available free of charge via the Internet at http://pubs.acs.org.

AUTHOR INFORMATION

Corresponding Author

*E-mail: zhugs@jlu.edu.cn.

Notes

The authors declare no competing financial interest.

ACKNOWLEDGMENTS

We are grateful to the financial support from National Basic Research Program of China (973 Program, Grants 2012CB821700), Major International (Regional) Joint Research Project of NSFC (Grants 21120102034) NSFC (Grants 20831002) and Australian Research Council Future Fellowship (FT100101059).

REFERENCES

(1) Whitesides, G. M. *Nat. Biotechnol.* **2003**, *21*, 1161−5.
(2) Emerich, D. F.; Thanos, C. G. *Expert Opin. Biol. Ther.* **2003**, *3*, 655−663.

(3) Davis, M. E.; Chen, Z. G.; Shin, D. M. *Nat. Rev. Drug. Discov.* **2008**, *7*, 771−82.
(4) Ruth, D. *Mater. Today* **2005**, *8*, 16−17.
(5) Peer, D.; Karp, J. M.; Hong, S.; Farokhzad, O. C.; Margalit, R.; Langer, R. *Nat. Nano* **2007**, *2*, 751−760.
(6) Wagner, V.; Dullaart, A.; Bock, A. K.; Zweck, A. *Nat. Biotechnol.* **2006**, *24*, 1211−7.
(7) Greco, F.; Vicent, M. J. *Adv. Drug Delivery Rev.* **2009**, *61*, 1203−1213.
(8) Vivero-Escoto, J. L.; Slowing, I. I.; Trewyn, B. G.; Lin, V. S. Y. *Small* **2010**, *6*, 1952−1967.
(9) Vallet-Regí, M.; Balas, F.; Arcos, D. *Angew. Chem., Int. Ed.* **2007**, *46*, 7548−7558.
(10) Wu, S.-H.; Hung, Y.; Mou, C.-Y. *Chem. Commun.* **2011**, *47*, 9972−9985.
(11) Lai, C.-Y.; Trewyn, B. G.; Jeftinija, D. M.; Jeftinija, K.; Xu, S.; Jeftinija, S.; Lin, V. S. Y. *J. Am. Chem. Soc.* **2003**, *125*, 4451−4459.
(12) Climent, E.; Bernardos, A.; Martínez-Máñez, R.; Maquieira, A.; Marcos, M. D.; Pastor-Navarro, N.; Puchades, R.; Sancenón, F. l.; Soto, J.; Amorós, P. *J. Am. Chem. Soc.* **2009**, *131*, 14075−14080.
(13) Patel, K.; Angelos, S.; Dichtel, W. R.; Coskun, A.; Yang, Y.-W.; Zink, J. I.; Stoddart, J. F. *J. Am. Chem. Soc.* **2008**, *130*, 2382−2383.
(14) Du, J.-Z.; Du, X.-J.; Mao, C.-Q.; Wang, J. *J. Am. Chem. Soc.* **2011**, *133*, 17560−17563.
(15) Aznar, E.; Marcos, M. D.; Martínez-Máñez, R. n.; Sancenón, F. l.; Soto, J.; Amorós, P.; Guillem, C. *J. Am. Chem. Soc.* **2009**, *131*, 6833−6843.
(16) Liu, R.; Zhang, Y.; Zhao, X.; Agarwal, A.; Mueller, L. J.; Feng, P. *J. Am. Chem. Soc.* **2010**, *132*, 1500−1501.
(17) Angelos, S.; Khashab, N. M.; Yang, Y.-W.; Trabolsi, A.; Khatib, H. A.; Stoddart, J. F.; Zink, J. I. *J. Am. Chem. Soc.* **2009**, *131*, 12912−12914.
(18) Meng, H.; Xue, M.; Xia, T.; Zhao, Y.-L.; Tamanoi, F.; Stoddart, J. F.; Zink, J. I.; Nel, A. E. *J. Am. Chem. Soc.* **2010**, *132*, 12690−12697.
(19) Zhao, Y.-L.; Li, Z.; Kabehie, S.; Botros, Y. Y.; Stoddart, J. F.; Zink, J. I. *J. Am. Chem. Soc.* **2010**, *132*, 13016−13025.
(20) Lee, C.-H.; Cheng, S.-H.; Huang, I. P.; Souris, J. S.; Yang, C.-S.; Mou, C.-Y.; Lo, L.-W. *Angew. Chem., Int. Ed.* **2010**, *49*, 8214−8219.
(21) Muhammad, F.; Guo, M.; Qi, W.; Sun, F.; Wang, A.; Guo, Y.; Zhu, G. *J. Am. Chem. Soc.* **2011**, *133*, 8778−8781.
(22) Mei, X.; Luo, X.; Xu, S.; Xu, D.; Zheng, Y.; Xu, S.; Lv, J. *Chem. Biol. Interact.* **2009**, *181*, 316−321.
(23) Fiallo, M. M. L.; Garnier-Suillerot, A. *Biochemistry* **1986**, *25*, 924−930.
(24) Kheirolomoom, A.; Mahakian, L. M.; Lai, C.-Y.; Lindfors, H. A.; Seo, J. W.; Paoli, E. E.; Watson, K. D.; Haynam, E. M.; Ingham, E. S.; Xing, L.; Cheng, R. H.; Borowsky, A. D.; Cardiff, R. D.; Ferrara, K. W. *Mol. Pharm* **2010**, *7*, 1948−1958.
(25) Abraham, S. A.; Edwards, K.; Karlsson, G.; MacIntosh, S.; Mayer, L. D.; McKenzie, C.; Bally, M. B. *Biochim. Biophys. Acta* **2002**, *1565*, 41−54.
(26) Fiallo, M. M. L.; Garnier-Suillerot, A.; Matzanke, B.; Kozlowski, H. *J. Inorg. Biochem.* **1999**, *75*, 105−115.